Journal of Chemistry and Technologies, 2023, *31*(3), 493-506

Journal of Chemistry and Technologies

pISSN 2663-2934 (Print), ISSN 2663-2942 (Online).

journal homepage: http://chemistry.dnu.dp.ua

UDC 547.77+541.49+546.562+539.26

$CuBr_2$ AS A BROMINATION AGENT OF PYRAZOLE-BASED LIGAND: SYNTHESIS OF COPPER(II) COORDINATION COMPOUNDS BY OXIDATIVE DISSOLUTION OF COPPER POWDER IN ORGANIC SOLVENTS

Oleksandr S. Vynohradov[1*], Yuliya M. Davydenko[1], Vadim O. Pavlenko[1], Dina D. Naumova[1], Igor O. Fritsky[1], Sergiu Shova[2], Olena V. Prysiazhna[3]

[1]*Department of Chemistry, Taras Shevchenko National University of Kyiv, Volodymyrska str. 64/13, 01601 Kyiv, Ukraine*

[2]*Poni Petru Institute of Macromolecular Chemistry, Aleea Gr. Ghica, Voda 41A, 700487 Iasi, Romania*

[3]*V. Bakul Institute for Superhard Materials of the National Academy of Sciences of Ukraine, Avtozavodskaya str. 2, 04074 Kyiv, Ukraine*

Received 5 June 2023; accepted 15 August 2023; available online 25 October 2023

Abstract

Using the direct synthesis method, by oxidative dissolution of copper powder in the presence of $CuBr_2$ and $C_5H_8N_2$ (3,5-dimethyl-1H-pyrazole), three different types of crystals were formed, isolated, and identified. Three new coordination compounds, trinuclear $[Cu_3(\mu_3\text{-}OH)(\mu_2\text{-}C_5H_7N_2Br)(\mu_2\text{-}Br)_3(C_5H_8N_2)_5Br]\cdot CHCl_3$ (where $C_5H_7N_2Br$ – 4-bromo-3,5-dimethylpyrazole) (1) (orthorhombic, *Pnma*), binuclear $[Cu_2(\mu_2\text{-}C_5H_7N_2Br)(\mu_2\text{-}Br)(C_5H_8N_2)_4Br_2]\cdot 2CHCl_3$ (2) (monoclinic, *C*2/c) and mononuclear $[CuBr_2(C_5H_8N_2)_3]$ (3) (triclinic, $P\bar{1}$), have been obtained. According to the single-crystal X-ray diffraction analysis, the complex 1 is a trinuclear six-membered cycle, where copper atoms are connected by three types of bridges: μ_2-bromide ions, μ_2-4-bromo-3,5-dimethylpyrazole molecule, and μ_3-hydroxo group. The binuclear complex 2 is formed due to a connection between two copper atoms by a bidentate-bridging bromide ion and a bridged 4-brominated 3,5-dimethylpyrazole molecule. Coordination compound 3 is a mononuclear trigonal-bipyramidal copper(II) complex. During the reaction, some part of 3,5-dimethylpyrazole molecules was brominated in the 4th position of the pyrazole ring. The Hirshfeld surface analysis reveals that the intermolecular H···H contacts have the highest contribution to the crystal packing of all compounds: 66.9 % for 1, 54.4 % for 2, and 66.5 % for 3.

Keywords: Copper complexes; pyrazole; bromination; direct synthesis; oxidative dissolution; Hirshfeld surface analysis; crystal structure; fractional crystallization.

$CuBr_2$ ЯК БРОМУЮЧИЙ АГЕНТ ПІРАЗОЛЬНИХ ЛІГАНДІВ: СИНТЕЗ КООРДИНАЦІЙНИХ СПОЛУК КУПРУМУ(II) ШЛЯХОМ ОКИСНОГО РОЗЧИНЕННЯ МІДНОГО ПОРОШКУ В ОРГАНІЧНИХ РОЗЧИННИКАХ

Олександр С. Виноградов[1], Юлія М. Давиденко[1], Вадим О. Павленко[1], Діна Д. Наумова[1], Ігор О. Фрицький[1], Сергій Шова[2], Олена В. Присяжна[3]

[1]*Київський національний університет імені Тараса Шевченка, вул. Володимирська, 64/13, Київ 01601, Україна*

[2]*Інститут макромолекулярної хімії "Петру Поні" Румунської АН, алея Грігоре Гіка Вода, 41-А, Яси 700487, Румунія*

[3]*Інститут надтвердих матеріалів ім. В.М. Бакуля НАН України, вул. Автозаводська, 2, Київ 04074, Україна*

Анотація

Методом прямого синтезу – окисним розчиненням мідного порошку в присутності $CuBr_2$ і $C_5H_8N_2$ (3,5-диметил-1Н-піразол) було виділено та ідентифіковано три різні типи кристалів. Отримано три нові координаційні сполуки, а саме триядерну $[Cu_3(\mu_3\text{-}OH)(\mu_2\text{-}C_5H_7N_2Br)(\mu_2\text{-}Br)_3(C_5H_8N_2)_5Br]\cdot CHCl_3$ (де $C_5H_7N_2Br$ – 4-бром-3,5-диметилпіразол) (1) (орторомбічна, *Pnma*) біядерну $[Cu_2(\mu_2\text{-}C_5H_7N_2Br)(\mu_2\text{-}Br)(C_5H_8N_2)_4Br_2]\cdot 2CHCl_3$ (2) (моноклінна, *C*2/c) та моноядерну $[CuBr_2(C_5H_8N_2)_3]$ (3) (триклінна, $P\bar{1}$). Згідно з результатами рентгеноструктурного аналізу, комплекс 1 є триядерним шестичленним циклом, де атоми купруму з'єднані між собою трьома типами містків: μ_2-бромід-іонами, молекулою μ_2-4-бром-3,5-диметилпіразолу та μ_3-гідроксогрупою. Біядерний комплекс 2 формується сполученням двох атомів купруму бідентатно-містковим бромід-іоном та містковою молекулою бромованого у 4-е положення 3,5-диметилпіразолу. Координаційна сполука 3 є моноядерним тригонально-біпірамідальним комплексом купруму(II). Відбулося бромування певної частини молекул 3,5-диметилпіразолу в 4-е положення піразольного кільця. Згідно з результатами аналізу поверхні Хіршфельда, міжмолекулярні контакти H···H мають найбільший внесок у кристалічну упаковку всіх сполук: 66.9 % для 1, 54.4 % для 2 і 66.5 % для 3.

Ключові слова: комплекси купруму; піразол; бромування; прямий синтез; окисне розчинення, аналіз поверхні Хіршфельда; кристалічна структура; фракційна кристалізація.

**Corresponding author: e-mail: oleksandr.vynohradov@knu.ua*

Introduction

Synthesis methods, crystal structure, and properties of transition metal complexes with different nuclearity are important areas of chemical research due to their wide-ranging applications. [1–3]. Among the organic N,N-donor ligands, pyrazoles hold a special place in the formation of coordination compounds because they can create structures with diverse topologies [4–6]. Pyrazole and its derivatives are also used as ligands for the synthesis of coordination compounds with useful properties [7–10]. Pyrazole-containing copper complexes attract attention because they can form structures with different ranges of nuclearity: from mononuclear to polynuclear complexes [11–13]. Pyrazoles can act as bidentate ligands [14; 15], forming bridges in polynuclear structures. However, the N(1)–H group may not necessarily be coordinated by a metal atom, it can be coordinated in a monodentate mode [16; 17] and may act as a donor of hydrogen bonds. Many types of coordination compounds can be obtained by direct synthesis [18], which is based on the process of oxidative dissolution of metal with organic ligand in an organic solvent [19]. The reaction system usually consists of several components: an oxidizing agent, a chelating agent, and a solvent. The oxidizing agent is often atmospheric oxygen in the air, and the chelating agent is an organic ligand. In this case, the introduction of a copper(II) salt into the system deserves attention, since it can be one of the possible sources of anions and an additional oxidizing agent. It is known that copper(II) bromide can be used as a brominating agent in organic synthesis [20–24]. In this regard, a question arises: can copper(II) bromide function as a brominating agent in such a system?

We herein report the preparation of three copper(II) coordination compounds using the direct synthesis method, which is based on the oxidative dissolution of powdered metal in the presence of an organic ligand in organic solvents.

Experimental and methods

All chemical reagents were commercial products of reagent grade and used without further purification unless otherwise specified.

IR spectroscopy. IR spectra were recorded with a Perkin-Elmer Spectrum BX FT-IR in the range of 400–4000 cm^{-1} in KBr pellets.

Elemental analysis. The elemental (CHN) analysis was performed using a CHNOS analyzer vario MICRO cube Elementar. The result was reported as percent by weight of each element with a precision of ±0.30 %.

*Crystal structure determination for **1–3**.* The experimental data were obtained on an Xcalibur Eos diffractometer with CCD detector (Mo *K*α radiation λ =0.71073 Å, graphite monochromator) at room temperature (293 *K*). Data collection: CrysAlis PRO 1.171.40.53; cell refinement: CrysAlis PRO 1.171.40.53; data reduction: CrysAlis PRO 1.171.40.53 (Rigaku OD) [25]. The structures were solved by intrinsic phasing method and refined by least-squares minimization method with the help of ShelXT and SHELXL programs [26, 27] using the graphical interface Olex2 [28]. Analytical numeric absorption correction using a multifaceted crystal model based on expressions derived by R. C. Clark & J. S. Reid. [29]. Empirical absorption correction using spherical harmonics, implemented in SCALE3 ABSPACK scaling algorithm. Details of the data collection and processing, structure analysis and refinement are summarized in Table 1. The structures were deposited at the Cambridge Crystallographic Data Centre (nos. 2017051, 2017052, 2017053).

Table 1

Crystallographic data, details of data collection, and characteristics of data refinement for complexes 1–3

Complexes	**1**	**2**	**3**
Chemical formula	$C_{30}H_{47}Br_5Cu_3N_{12}O\cdot(CHCl_3)$	$C_{25}H_{38}Br_4Cu_2N_{10}\cdot 2(CHCl_3)$	$C_{15}H_{24}Br_2CuN_6$
M_r, g/mol	1301.33	1164.11	511.76
Crystal system	Orthorhombic	Monoclinic	Triclinic
Space group	*Pnma*	$C2/c$	$P\bar{1}$
a, Å	19.9353(8)	18.4331(13)	9.1353 (6)
b, Å	14.6342(8)	13.4024(6)	9.6978 (6)
c, Å	16.4342(7)	18.2358(9)	12.7716 (5)
α, deg	90	90	105.880 (4)
β, deg	90	94.231(4)	97.800 (5)
γ, deg	90	90	103.709 (5)
Volume, Å^3	4794.5(4)	4492.8(4)	1032.64 (11)
Z	4	4	2
T, *K*	293	293	293
ρ_{calcd}, mg/m^3	1.803	1.721	1.646

Continued in Table 1

μ, mm^{-1}	5.69	4.89	4.94
F (000)	2556	2288	510
θ range, deg	1.6 to 25.0	1.9 to 25.0	1.8 to 27.4
Measured reflections	12262	10174	7809
Independent reflections	4418	5211	4720
Reflections with I > 2σ(I)	2891	2767	3284
R_{int}	0.05	0.046	0.023
$\Delta\rho_{max}$, $\Delta\rho_{min}$, *e* Å^{-3}	3.40, −0.62	1.13, −0.56	0.69, −0.64
$R[F^2 > 2\sigma(F^2)]$	0.062	0.063	0.045
$wR(F^2)$	0.180	0.152	0.093
h	−16→23	−17→25	−9→12
k	−17→13	−18→17	−13→12
l	−19→13	−24→17	−14→17
Crystal size, mm	0.5 × 0.2 × 0.2	0.7 × 0.1 × 0.08	0.6 × 0.5 × 0.3

The Hirshfeld surface analysis. The Hirshfeld surface analysis and the associated two-dimensional fingerprint plots were performed using Crystal Explorer 17.5 software [30], with a standard resolution of the three-dimensional d_{norm} surfaces (high resolution, isovalue 0.5) plotted over a fixed colour scale of –0.1218 (red) to 1.5377 (blue) a.u. for trinuclear complex **1**, –0.2682 (red) to 1.4773 (blue) a.u. for dinuclear complex **2**, and **–**0.3449 (red) to 1.5228 (blue) a.u. for mononuclear complex **3**. Fingerprint breakdown: Filtering fingerprint by element type. The surface area included (as a percentage of the total surface area) for close contacts between atoms inside and outside the surface. Filtered fingerprint plots are produced by applying a filter to highlight only close contacts between pairs of atoms of particular chemical elements. Only contributions from those contacts are shown in the fingerprint plot, with the rest greyed out.

Synthesis of 3,5-dimethyl-1H-pyrazole. Hydrazine hydrate 24 ml (90 %, 25.03 g, 0.5 mol), previously cooled to 10 °C was added dropwise slowly (within 30 min) to 51.2 ml (50 g; 0.5 mol) of acetylacetone, dissolved in 400 ml of ethanol (Scheme). The reaction was carried out with constant stirring and cooling. The reaction mixture was stirred for 3 hours and left overnight. The ethanol was distilled off and light yellow crystals were obtained, which were washed with cold ethanol and dried in air. The yield of the crystalline product was 75 %. ^{1}H NMR (DMSO-d_6), δ: 2.14 (s., 6H; 2CH_3), 5.64 (s., 1H; pz-CH), 11.87 (br. s., 1H; NH). Elemental analysis: calculated (%): C 62.47; H 8.39; N 29.14. Found: C 62.49; H 8.33; N 29.16.

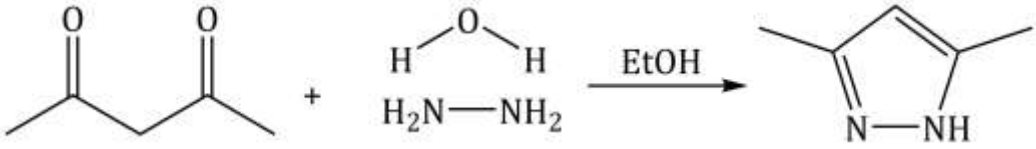

Scheme. Synthesis of 3,5-dimethyl-1H-pyrazole

*Synthesis of **1–3**.* Complexes were synthesized as a result of the addition of a solution of 1.35 g (14.06 mmol) of 3,5-dimethyl-1*H*-pyrazole in methanol (10 ml) to a mixture of copper metal (0.6 g, 9.37 mmol) and $CuBr_2$ (1.05 g, 4.68 mmol). The reaction mixture was magnetically stirred at ambient temperature for 1 hour in the air until precipitation of the product. The dark green precipitate was filtered off and dissolved in chloroform. Single crystals suitable for X-ray analysis were obtained by slow evaporation of the solvent at room temperature in an open vessel via fractional crystallization. As a result of the slow evaporation from the red-brown solution, dark blue crystals of $C_{30}H_{47}Br_5Cu_3N_{12}O\cdot(CHCl_3)$ (**1**) first precipitated. After removing them, the solution color turned green, and a small amount of dark green needle crystals of the complex $C_{25}H_{38}Br_4Cu_2N_{10}\cdot2(CHCl_3)$ (**2**) fell out. Finally, a small amount of green crystals of the $C_{15}H_{24}Br_2CuN_6$ (**3**) was isolated. The yield was 1.8 g (81%). Yields of complexes **2** and **3** are insignificant and do not exceed 5%.

Results and Discussion

The interaction process in the studied system can be described by the following sequence of reactions:

Stage 1 – the formation of a Cu^{2+} pyrazole-based complex, which determines the initial color of the solution.

Stage 2 – oxidation by dissolving of metallic copper powder by reaction (1) and the formation of Cu^{1+} complexes.

$Cu^0 + Cu^{2+} = 2Cu^{1+}$ (1)

It is reasonable to assume that the formation of polynuclear Cu^{1+} will occur, where bromide ions will act as bridging ligands Based on the results described below, it is presumed that a six-membered trinuclear monovalent copper complex is formed initially.

Stage 3 – the monovalent complex is oxidized by atmospheric oxygen with the formation of some superoxo- and peroxoparticles (2a, 2b, 2c):

$Cu^{1+} + O_2 = Cu^{2+} + O_2$ (2a)

$2Cu^{1+} + O_2 = Cu^{2+} + O_2^{2-}$ (2b)

$2O_2^{\cdot-} = O_2 + O_2^{2-}$ (2c)

This fact explains the formation of free bromine (3a), which then reacts with some of the 3,5-dimethylpyrazole molecules in the 4th position (3b). This process facilitates the deprotonation of the organic ligand molecule and promotes the realization of bridging functions.

$O_2^{2-} + 2Br^- = 2O^{2-} + Br_2$ (3a)

$Br_2 + C_5H_8N_2 = C_5H_7N_2Br + HBr$ (3b)

Considering the results of elemental analysis and IR spectroscopy, the general chemical equation between copper powder, copper(II) bromide and 3,5-dimethyl-1H-pyrazole in methanol can be written as:

$$1Cu + 5CuBr_2 + 12C_5H_8N_2 + O_2 = 2[Cu_3(OH)(C_5H_7N_2Br)(C_5H_8N_2)_5Br_4]. \quad (4a)$$

Complexes **2** and **3** are formed during the dissolution stage of the complex **1** precipitate in chloroform, which also contains a residual amount of metallic copper powder.

IR spectra and elemental analysis. The IR spectra of the ligand and the dark green precipitate were recorded and analyzed (Fig. 1). The following characteristic IR absorbance peaks can be observed in the IR spectrum of the ligand (spectrum 1): 3202, 3132, 3110, 3039, 2992, 2945, 2879, 2788, 2607, 1666, 1595, 1484, 1422, 1306, 1154, 1028, 855, 779, 736, 661, and 403 cm^{-1}. The ν_{X-H} bands are presented in the range of 3300–2800 cm^{-1}. The IR spectrum of 1 shows an absorption band centered at 3202 cm^{-1} characteristic of an N–H stretching vibration. The ν(C–H) absorption band is observed at 3132 cm^{-1} while ν_{asym}(C–H) stretching vibrations are identified at 3039, 2945, 2879, and 2788 cm^{-1}. Very weak peaks at 2607 and 1666 cm^{-1} can be described as CH overtones/combinations. The CC stretch vibrations are as a strong absorption band at 1595 cm^{-1} in the spectrum 1. The strong sharp band at 661 cm^{-1} is the N-C-C *out* of *plane bending* vibrations. This type of bending takes plane outside of the plane of the molecule. The strong sharp band at 403 cm^{-1} is C-CH_3 vibrations (in-plane bending type) [31]. In these types of vibrations, there is a change in bond angle. This type of bending takes place within the same plane.

There are the next characteristic IR absorbance peaks in the IR spectrum of the dark green precipitate (spectrum 2): 3465, 3350, 3294, 3094, 3019, 2967, 2923, 2857, 1571, 1472, 1410, 1288, 1178, 1149, 1044, 985, 889, 845, 799, 669, 654, 584, 562, 460 and 435 cm^{-1}. Two small peaks at 3465 and 3350 cm^{-1} confirm the presence of OH groups in the composition of the test sample. The absorption band at 3465 cm^{-1} is overlapped with the intensity absorption band of NH valence oscillations at 3294 cm^{-1}, which confirms the presence of 3,5-dimethyl-1H-pyrazole coordinated in a monodentate mode. The shift of the absorption band in comparison with its position in the spectrum of the ligand is 92 cm^{-1}. The absorption bands in the range of 3100-2850 cm^{-1} were assigned to CH stretching vibrations. Several medium absorption bands from 630 to 550 cm^{-1} due to C-Br stretching vibrations of brominated 3,5-dimethylpyrazole. These bands are absent in the spectrum of free organic ligand.

The results of elemental analysis correspond to the composition of $C_{30}H_{47}Br_5Cu_3N_{12}O$: found (%) C 30.87, H 4.03, N 13.87; calculated for $C_{30}H_{47}Br_5Cu_3N_{12}O$ (%): C 30.49, H 4.0, N 14.22. The results of elemental analysis of the dark green precipitate obtained after dissolving the reagents in methanol and single crystals of complex **1** were identical. Obviously, dissolving the precipitate in chloroform does not affect the structure of complex **1**.

Description of the complexes. The structure **1** (Fig. 2) consists of trinuclear six-membered molecules, centered by the tridentate bridging OH group. The plane of symmetry passes through the Br1, O1, Cu2, Br3, N6, N7 C14, C15, C16, C17 and C18 atoms and divides the molecule into two equal parts. An isosceles triangle (Br1⋯Br2 = Br1⋯$Br2^i$ = 5.7891(14) Å, Br2⋯$Br2^i$ = 4.820(2) Å, Br1–Br2–$Br2^i$ = Br2–$Br2^i$–Br1 = 65.401(11)°, Br2–Br1–$Br2^i$ = 49.2(2)°) is the basis of the metallocycle where copper atoms are connected by μ_2-bromide ions which are located at its vertices. Intermetallic distance between.

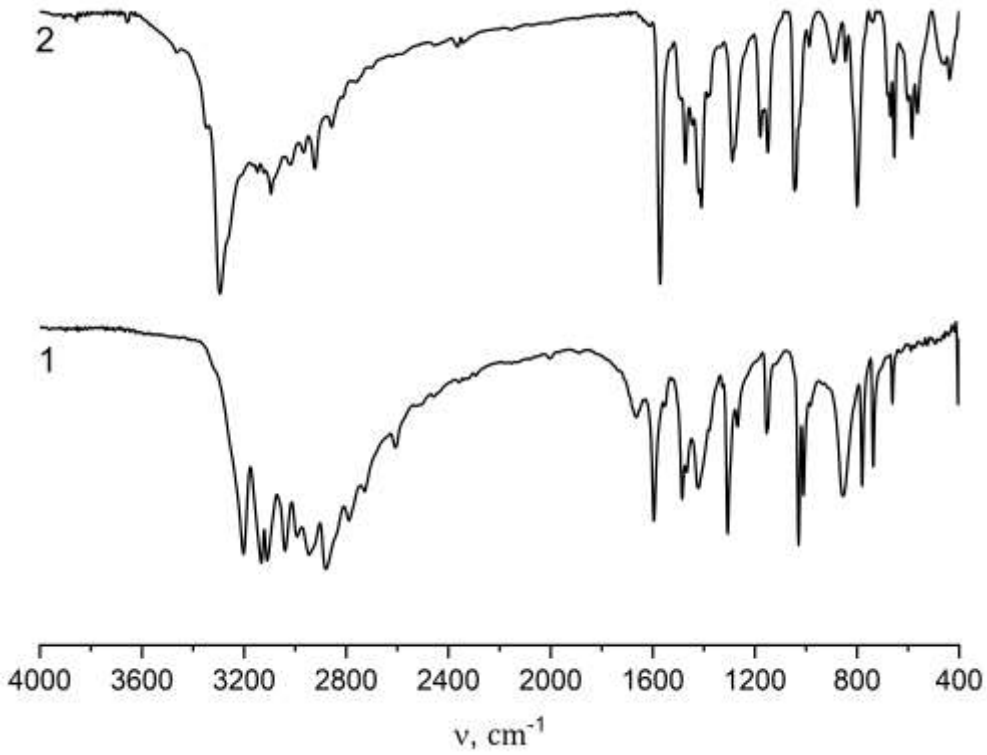

Fig. 1. IR spectra of 3,5-dimethyl-1H-pyrazole (1) and the dark green precipitate (2) obtained after 1 hour of mixing the initial reagents

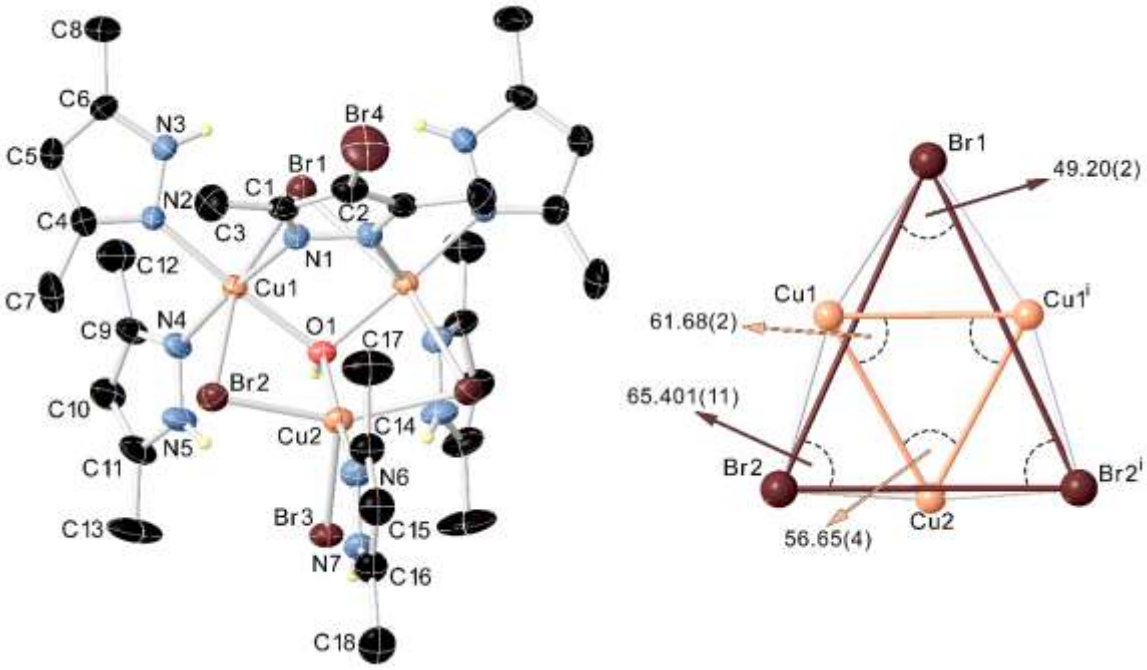

Fig. 2. The molecular structure of 1 and the structure of the six-membered metallocycle of the complex. A non-coordinated solvent molecule and irrelevant hydrogen atoms are omitted for clarity. Symmetry code: (i) +*x*, ½-*y*, +*z*

Cu1···Cu1^{i} and Cu1···Cu2 are 3.208(2) and 3.3809(16) Å, respectively (symmetry code: (i) +*x*, ½-*y*, +*z*). As a result of deprotonation, one pyrazole ligand molecule was converted into a pyrazolate anion, which binds Cu1 and Cu1^{i} atoms in a bidentate-bridging mode. During the reaction, this μ_2-3,5-dimethylpyrazole was brominated in the 4th position (C2–Br4 = 1.870(12) Å). The μ_3-OH group asymmetrically binds copper atoms and leaves the metalocyclic plane by 0.644(6) Å, from the μ_2-Br atoms plane by 0.810(6) Å. The Cu1 atom has a distorted tetragonal-bipyramidal

coordination environment formed by two nitrogen atoms of different protonated molecules of 3,5-dimethylpyrazole, μ_3-O atom, two μ_2-Br ions in axial positions, and is supplemented by a bridged 4-bromo-3,5-dimethylpyrazole molecule. The geometric environment distortion of Cu1 atom towards the elongated tetragonal-bipyramid, which is typical for copper complexes. The Cu–Br axial bonds are longer than the equatorial bonds, while the last ones (Cu–O and Cu–N) are almost identical. The distorted square-pyramidal geometry of the five-coordinated Cu2 atom (τ_5(Cu2) = 0.295) [32], is realized by three bromide ions, one of them is at the top of the pyramid, and the other two perform bridging functions, the nitrogen atom of the protonated 3,5-dimethylpyrazole molecule and O atom from μ_3-OH group. X-ray single crystal analysis of complex **1** confirmed the existence of four metalocyclic molecules in one unit cell. The crystal structure (Fig. 3) is formed by the neutral trinuclear molecules arranged within the unit cell in two rows along the *a*-axis direction. These molecules are connected to each other by a wide system of H-bonds. The molecules are connected by mostly electrostatic intramolecular CH···N and NH···Br hydrogen bonds (Table 2).

The strong hydrogen bonds in this structure are not identified.

Table 2

Intramolecular hydrogen-bond geometry of complex 1 (Å, °)

D–H···A	D–H	H···A	D···A	D–H···A
C12–H12A···N2	0.959	2.512	3.187(12)	127.4
N3–H3···Br1	0.861	2.707	3.302(7)	127.4
N7–H7···Br3	0.859	2.820	3.397(10)	125.9
N5–H5···Br2	0.860	2.869	3.386(7)	120.4
C3–H3A···N3	0.959	2.866	3.456(12)	120.8

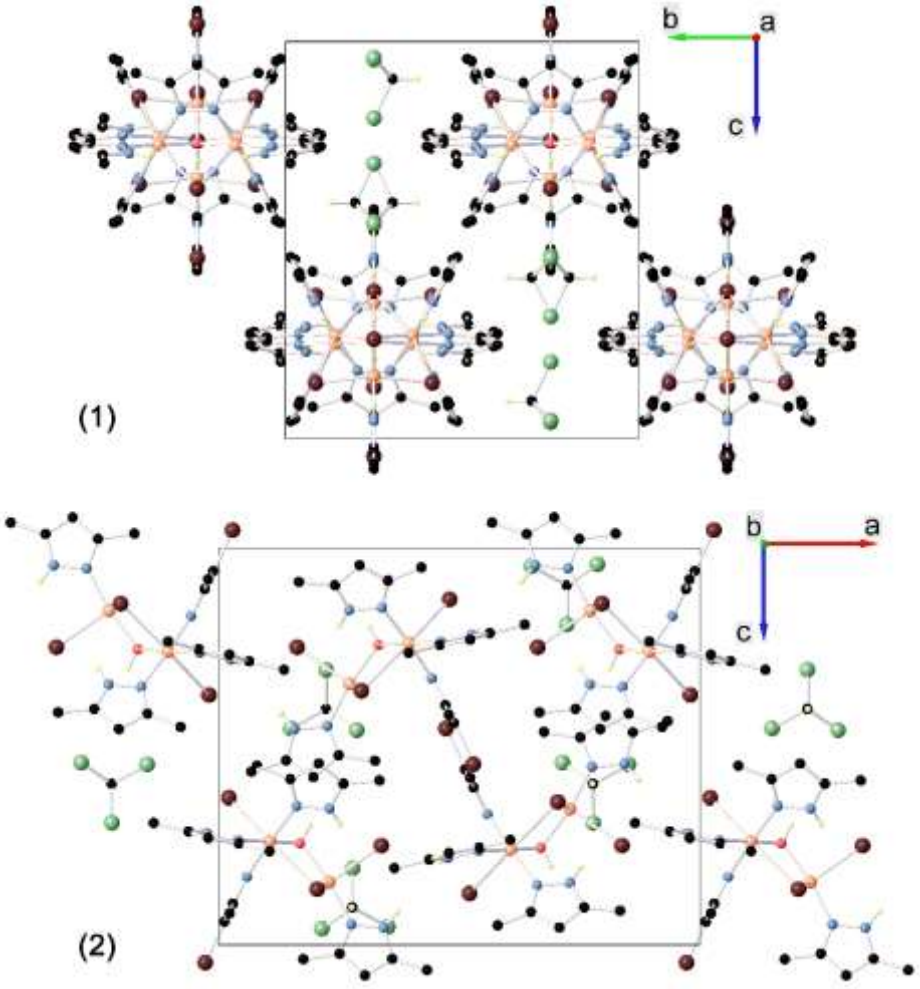

Fig. 3. Crystal packing of 1 viewed along the *a*- (1) and *b*-axis (2) directions. Irrelevant hydrogen atoms are not shown

Selected bond lengths and bond angles of complex **1** are shown in Table 3.

Table 3

*Selected bond lengths (Å) and bond angles (°) of complex **1***

Bond lengths (Å)			
Cu1–Br1	2.9549(14)	Cu2–Br2	2.4770(10)
Cu1–Br2	2.8968(13)	Cu2–Br3	2.6449(19)
Cu1–O1	2.034(4)	Cu2–O1	2.010(7)
Cu1–N1	1.976 (6)	Cu2–N6	1.974 (9)
Cu1–N2	1.999(7)	C2–Br4	1.869(12)
Cu1–N4	2.020(6)	Cu1···Cu2	3.3809(16)
Cu1···Cu1^{i}	3.208(2)	Cu1^{i}···Cu2	3.3809(16)
Bond angles (°)			
Br2–Cu1–Br1	163.22(5)	Br2–Cu2–Br2^{i}	153.25(8)
O1–Cu1–Br1	87.02(16)	Br2^{i}–Cu2–Br3	103.33(4)
O1–Cu1–Br2	77.22(16)	Br2–Cu2–Br3	103.33(4)
N1–Cu1–Br1	85.56(18)	O1–Cu2–Br2	88.54(6)
N1–Cu1–Br2	87.17(18)	O1–Cu2–Br2^{i}	88.54(6)
N1–Cu1–O1	84.4(3)	O1–Cu2–Br3	91.8(2)
N1–Cu1–N2	92.8(3)	N6–Cu2–Br2^{i}	89.37(8)
N1–Cu1–N4	175.2(3)	N6–Cu2–Br2	89.37(8)
N2–Cu1–Br1	90.71(19)	N6–Cu2–Br3	97.3(3)
N2–Cu1–Br2	104.7(2)	N6–Cu2–O1	171.0(4)
N2–Cu1–O1	176.5(2)	Cu1–O1–Cu1^{i}	104.1(3)
N2–Cu1–N4	91.9(3)	Cu2–O1–Cu1^{i}	113.4(2)
N4–Cu1–Br1	95.3(2)	Cu2–O1–Cu1	113.4(2)
N4–Cu1–Br2	90.72(19)	Cu2–Br2–Cu1	77.54(4)
N4–Cu1–O1	91.0(3)		
Symmetry code: (i) +*x*, ½-*y*, +*z*			

A five-membered bimetallic cycle of compound **2** (Fig. 4.) is formed by two copper atoms connected by a bridged 4-bromo-3,5-dimethylpyrazole molecule and a μ_2-Br ion. The distance between copper atoms is larger than the same distance in complex **1** by 0.58 Å (Cu1 ⋯ Cu2 = 3.7883(15) Å) and correlates with the literature data about similar complexes (for example, Cu1⋯Cu2 = 3.687 Å, [33]).

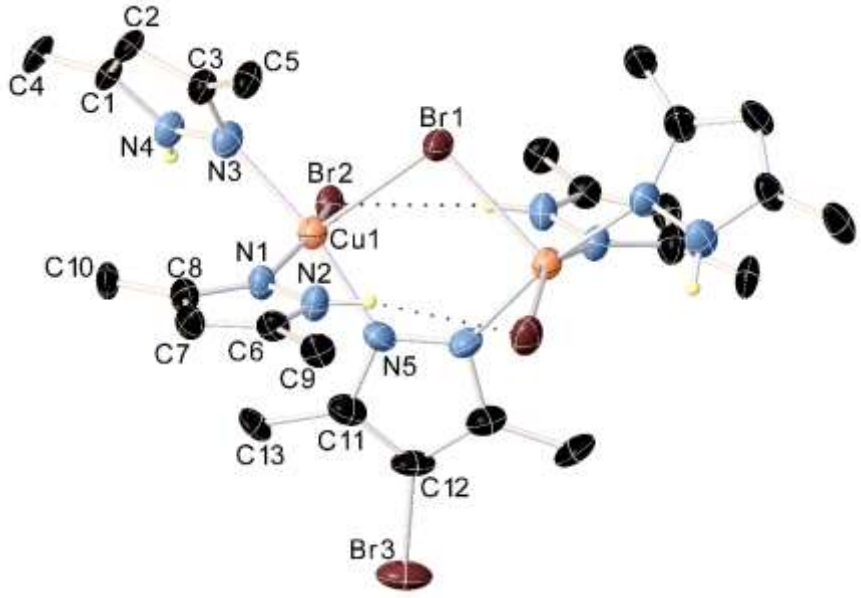

Fig. 4. Molecular structure of 2. Irrelevant hydrogen atoms and non-coordinated solvent molecules are not shown

The C–Br bond length in the brominated pyrazole ring practically does not change compared to the same bond length in complex **1** (C12–Br3 = 1.887(9) Å, the difference is 0.018 Å). The C_2 axis passes through the Br1, C12, and Br3 atoms and divides the 4-bromo-3,5-dimethylpyrazole bridged molecule and the whole complex molecule into two symmetrical parts. Both copper atoms are in a distorted square-pyramidal geometric environment

(τ_5(Cu1) = 0.205), which is formed by a nitrogen atom of μ_2-4-bromo-3,5-dimethylpyrazole, μ_2-Br ion, two nitrogen atoms of two 3,5-dimethyl-1*H*-pyrazoles and one terminal Br ion. The structure of complex **2** is further stabilized by intramolecular hydrogen bonds N2–H2···Br2^{i} = 2.5576 Å (N2–H2 = 0.860 Å, N2···Br2^{i} = 3.394(6) Å, N2–H2–Br2^{i} = 164.5°; (i) = 1-*x*, +*y*, ½-*z*). Selected bond lengths and bond angles of complex **2** are shown in Table 4. In crystal packing (Fig. 5) discrete [$Cu_2(\mu_2\text{-}C_5H_7N_2Br)(\mu_2\text{-}Br)(C_5H_8N_2)_4Br_2$] molecules arranged in chains, which are constructed due to the antisymmetric arrangement of brominated pyrazole planes of individual molecules along the *c*-axis direction. There are eight solvate chloroform molecules in one unit cell.

Table 4

Selected bond lengths (Å) and bond angles (°) of complex 2

Bond lengths (Å)			
Cu1–Br1	2.5733(10)	Cu1–N5	1.970(5)
Cu1–Br2	2.5110(10)	C12–Br3	1.887(9)
Cu1–N1	2.035(5)	Cu1···Cu1^{i}	3.7883(15)
Cu1–N3	2.012(5)		
Bond angles (°)			
Cu1^{i}–Br1–Cu1	94.80(5)	N5–Cu1–Br2	89.22(15)
Br2–Cu1–Br1	98.39(3)	N5–Cu1–N3	170.0(2)
N3–Cu1–Br1	95.85(15)	N5–Cu1–N1	88.8(2)
N3–Cu1–Br2	89.67(15)	N1–Cu1–Br1	103.94(16)
N3–Cu1–N1	88.4(2)	N1–Cu1–Br2	157.68(16)
N5–Cu1–Br1	94.19(14)		

Symmetry code: (i) −*x*+1, *y*, −*z*+1/2

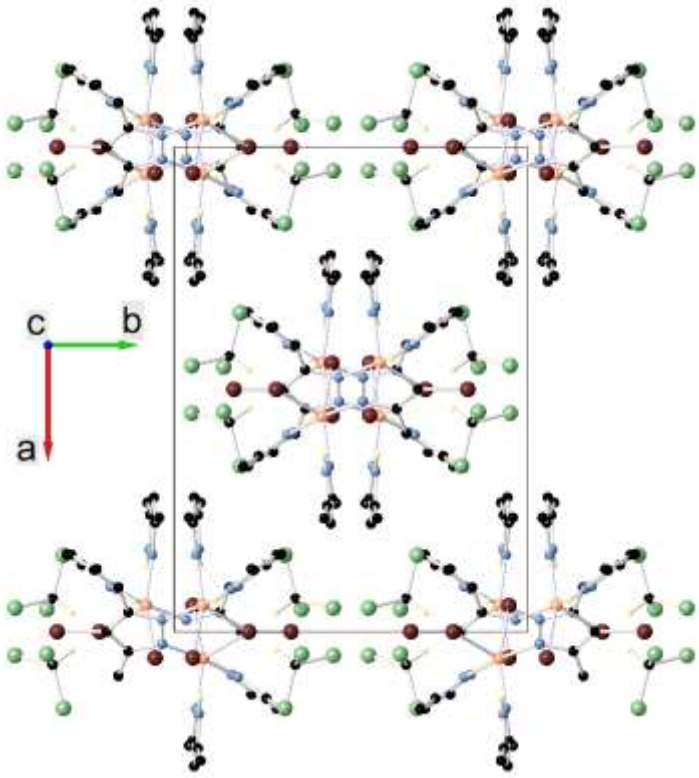

Fig. 5. The crystal structure of 2 along the c-axis. Irrelevant hydrogen atoms are not shown

In mononuclear copper(II) pyrazole-based complex **3** (Fig. 6) the central copper atom has coordination number 5 and trigonal-bipyramidal geometry (τ_5(Cu1) = 0.777). The equatorial plane is formed by Br1 and Br2 ions and the N2 atom of the 3,5-dimethyl-1H-pyrazole molecule. N1 and N3 atoms from the other two pyrazole molecules are in the axial position. The molecular structure of the complex is stabilized by intramolecular hydrogen bonds N6–H6···Br1 = 2.5826 Å (N6–H6 = 0.860 Å, N6···Br1 = 3.162(5) Å, N6–H6–Br1 = 125.6°) and N4–H4···Br2 = 2.5415 Å (N4–H4 = 0.860 Å, N4···Br2 = 3.131(4) Å, N6–H6–Br1 = 126.6°). Selected bond lengths (Å) and bond angles (°) of complex **3** are given in Table 5.

Journal of Chemistry and Technologies, 2023, *31*(3), 493-506

Table 5

Selected bond lengths (Å) and bond angles (°) of complex 3

Bond lengths (Å)			
Cu1–Br1	2.6368(7)	Cu1–N1	2.001(3)
Cu1–Br2	2.4910(7)	Cu1–N3	1.989(3)
Cu1–N2	2.044(3)		
Bond angles (°)			
Br2–Cu1–Br1	116.26(2)	N1–Cu1–N2	89.18(13)
N2–Cu1–Br1	111.64(9)	N3–Cu1–Br1	89.90(12)
N2–Cu1–Br2	132.02(9)	N3–Cu1–Br2	87.87(10)
N1–Cu1–Br1	91.10(10)	N3–Cu1–N2	89.61(14)
N1–Cu1–Br2	92.50(10)	N3–Cu1–N1	178.65(15)

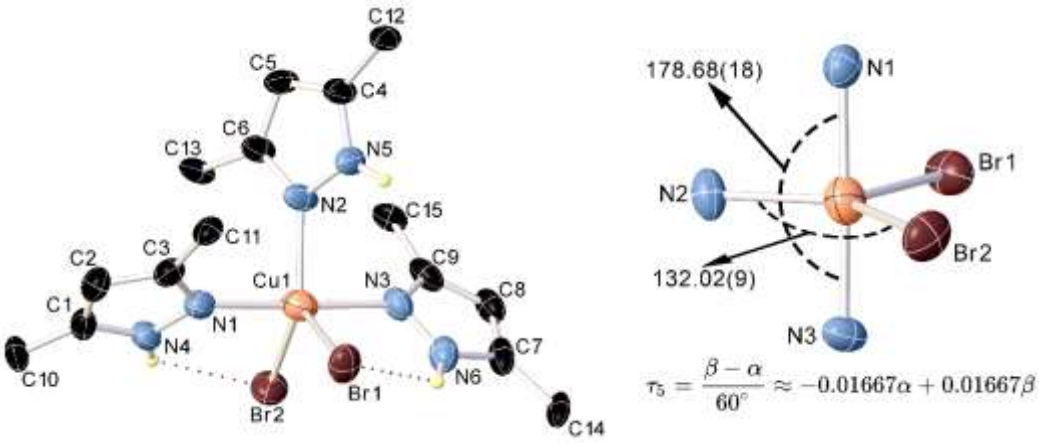

Figure 6. Molecular structure and coordination environment of Cu1 in complex 3. The formula for calculating the geometry index τ_5 is also given (β > α are the two greatest valence angles of the coordination center). Irrelevant hydrogen atoms are not shown

The crystal packing (Fig. 7) depicts a well-defined layer structure perpendicular to the *c*-axis direction.

Each layer consists of discrete molecules that are connected between each other by van der Waals interactions. These layers of molecules are connected by weak N–H···Br hydrogen bonds:

$N5^{i}$–$H5^{i}$···Br1 = 2.587 Å ($N5^{i}$–$H5^{i}$ = 0.860 Å, $N5^{i}$···Br1 = 3.403(2) Å, $N5^{i}$– $H5^{i}$–Br1 = 158.7°, (i) = 1-*x*, 1-*y*, -*z*). The equatorial Br1/Br2/N2 planes of the molecules are located parallel to the *b*-axis direction. The Cu···Cu intermetallic distance in the unit cell is 9.7479(12) Å.

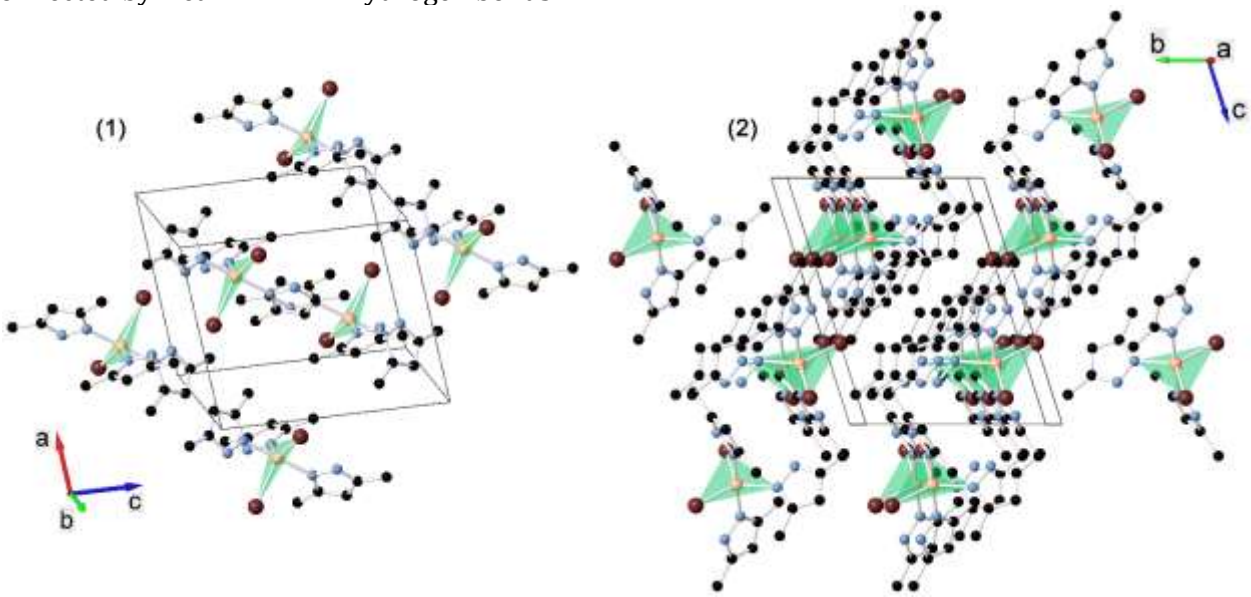

Fig. 7. Crystal structure of 3 with an illustration of the Br2/Br1/N2 equatorial plane placed parallel to the *b*-axis (1) and the symmetric arrangement of molecules along the *a*-axis (2). Hydrogen atoms are not shown

The Hirshfeld surface analysis. There are 14 red spots on the d_{norm} surface of trinuclear complex **1**, 8 red spots on the d_{norm} surface of dinuclear complex **2**, and only 5 red spots on the d_{norm} surface of mononuclear complex **3** (Fig. 8).

The dark red spots arise as a result of short interatomic contacts and represent negative d_{norm} values on the surface, while the other weaker intermolecular interactions appear as light-red spots.

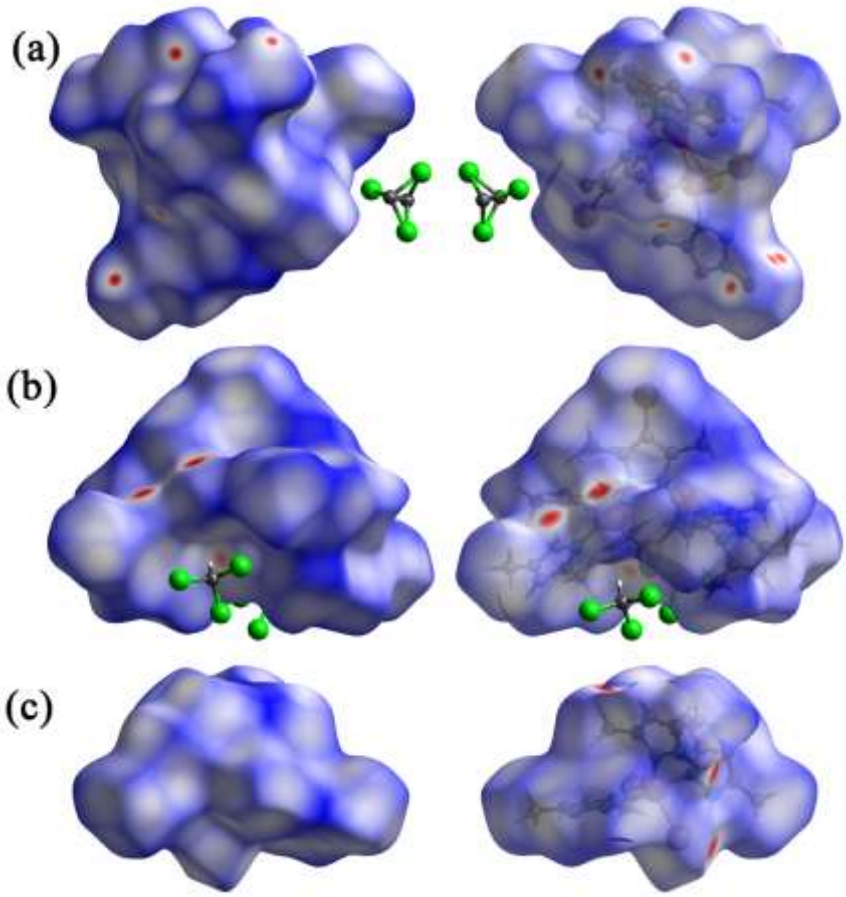

Fig. 8. Hirshfeld surface representations for complexes 1 (a), 2 (b), and 3 (c) with the function d_{norm} plotted onto the surface. Hydrogen atoms for 1 are not shown

For complex **1** the Hirshfeld surfaces mapped over d_{norm} are shown for the H···H, H···Br/Br···H, $H_{inside}\cdots Cl_{outside}$ (close contacts between the complex molecule and the solvent molecules), H···C/C···H, and H···N/N···H contacts. The overall two-dimensional fingerprint plot and the decomposed two-dimensional fingerprint plots are given in Fig. 9. The chloroform solvent molecules are the source of $H_{inside}\cdots Cl_{outside}$ close contacts. $CHCl_3$ molecules are outside the Hirschfeld surface and make close contacts with atoms inside the surface. The contribution of such contacts, in general, is 9.4%: $H_{inside}\cdots Cl_{outside}$ 7.2 %, $Br_{inside}\cdots Cl_{outside}$ 1.1 %, $C_{inside}\cdots Cl_{outside}$ 0.7 % та $N_{inside}\cdots Cl_{outside}$ 0.4 %. The most significant contributions to the overall crystal packing are from the same H···H (66.9 %), H···Br/Br···H (16.3 %), $H_{inside}\cdots Cl_{outside}$ (7.2 %), and H···C/C···H (4.9 %) contacts. The small contribution of the other weak intermolecular H···N/N···H (1.5 %), Cu···O/O···Cu (0.7%), Cu···H/H···Cu (0.7%), O···O (0.6 %), O···N/N···O (0.3%), O···C/C···O (0.3 %), and C···C (0.1 %) contacts has a negligible effect on the packing. Also, quantitative physical properties of the Hirshfeld surface for complex **1** were obtained, such as molecular volume (1061.34 $Å^3$), surface area (709.34 $Å^2$), globularity (0.709), as well as asphericity (0.005).

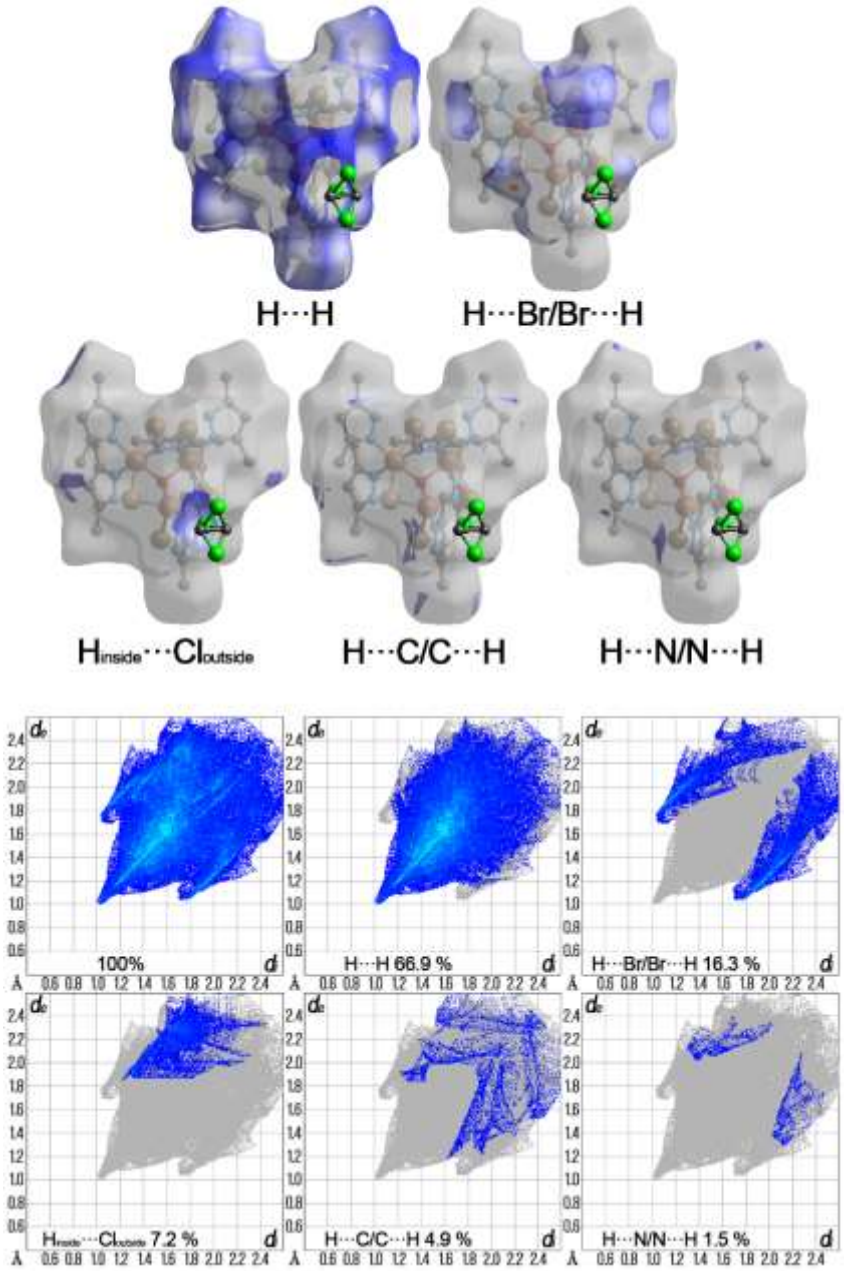

Fig. 9. Hirshfeld surface representations with the function d_{norm} plotted onto the surface for the different interactions, the overall two-dimensional fingerprint plot and those delineated into specified interactions for 1

For complex **2** the Hirshfeld surfaces mapped over d_{norm} are shown for the H···H (54.4%), H···Cl/Cl···H (17.6%), H···Br/Br···H (16%) and H···C/C···H (6.3%). Hirshfeld surface representations with the function d_{norm} plotted onto the surface for these interactions, the overall two-dimensional fingerprint plot and those delineated into specified interactions are shown in Fig. 10. The contribution of close contacts between the complex molecule and solvent molecules to the overall crystal packing is quite significant ($H_{inside}\cdots Cl_{outside}$ = 17.6%). There are also $Br_{inside}\cdots Cl_{outside}$ contacts, but their contribution is insignificant (2.4%). The contribution of H···N/N···H contacts is 1.7 %, $C_{inside}\cdots Cl_{outside}/Cl_{outside}\cdots C_{inside}$ = 1.1 %, $N_{inside}\cdots Cl_{outside}/Cl_{outside}\cdots N_{inside}$ = 0.4 %. The central copper atom does not participate in the formation of the Hirschfeld surface. It is worth noting the significant contribution to the total surface area of close contacts between the complex molecule and the solvent molecules. Quantitative physical properties of the Hirshfeld surface for complex **2** were obtained, such as molecular volume (871.63 Å^3), surface area (631.06 Å^2), globularity (0.699), as well as asphericity (0.045).

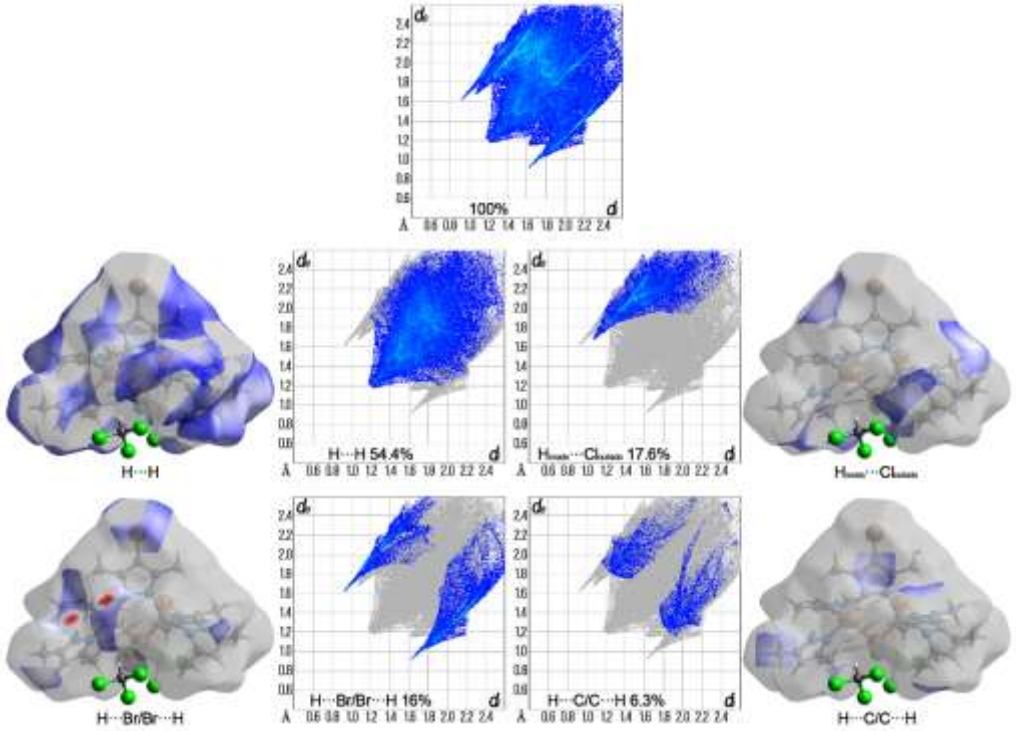

Fig. 10. Hirshfeld surface representations with the function d_{norm} plotted onto the surface for the different interactions, the overall two-dimensional fingerprint plot and those delineated into specified interactions for 2

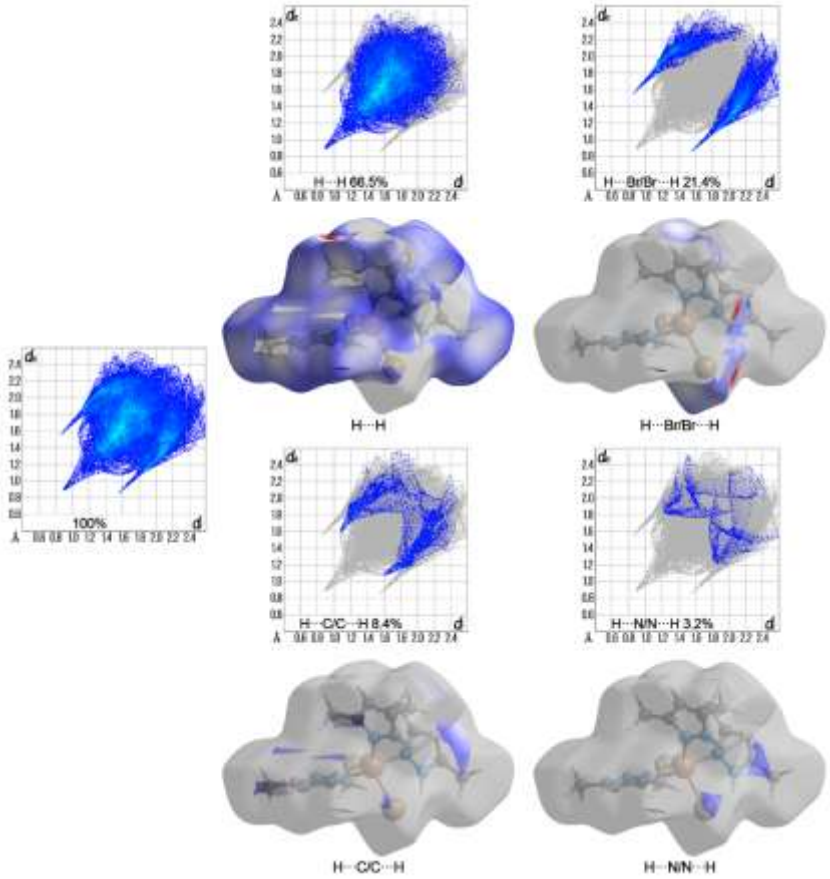

Fig. 11. Hirshfeld surface representations with the function d_{norm} plotted onto the surface for the different interactions, the overall two-dimensional fingerprint plot and those delineated into specified interactions for 3.

For complex **3** the largest contribution to the overall crystal packing comes from H···H interactions (66.5 %), which are located in the middle region of the fingerprint plot. H···Br/Br···H

contacts contribute 21.4 %, H···C/C···H – 8.4 %, H···N/N···H – 3.2%, Br···N/N···Br – 0.3 %, N···C/C···N – 0.1 % and C···C contacts contribute 0.1 % to the Hirshfeld surface. The central copper atom does not participate in the formation of the Hirschfeld surface. Hirshfeld surface representations with the function d_{norm} plotted onto the surface for these interactions, the overall two-dimensional fingerprint plot and those delineated into specified interactions are shown in Fig. 11. Quantitative physical properties of the Hirshfeld surface for complex **3** were obtained: molecular volume (508.16 Å^3), surface area (408.87 Å^2), globularity (0.753), as well as asphericity (0.059).

Conclusions

Three copper(II) pyrazole-based coordination compounds have been obtained through fractional crystallization using the oxidative dissolution of copper powder in organic solvents. The presented compounds are an example of the diversity of coordination properties exhibited by copper as a central atom, which can form complexes with different nuclearities and coordination polyhedra as a square-pyramidal, a trigonal-bipyramidal, and a tetragonal-bipyramidal. Copper bromide acted as a brominating agent in the presence of copper powder and organic solvent, resulting in the bromination of the ligand molecules. Taking into account the results of the elemental analysis, it was proved that there is no influence of the solvent on the formation of the six-membered trinuclear structure of complex **1**. The presence of OH groups and a 3,5-dimethyl-1H-pyrazole coordination in a monodentate mode was confirmed by IR spectroscopy. Hirshfeld surface analysis of the intermolecular contacts reveals that the most significant contributions to the overall crystal packing of all complexes are from H···H contacts. The value of asphericity increases with decreasing the nuclearity, while the globularity does not depend on the nuclearity of complexes.

Funding information

This work was supported by the Ministry of Education and Science of Ukraine (grant No. 22BF037-09 at Taras Shevchenko National University of Kyiv).

References

[1] Malinowski, J., Zych, D., Jacewicz, D., Gawdzik, B., Drzeżdżon, J. (2020). Application of Coordination Compounds with Transition Metal Ions in the Chemical Industry–A Review. *International Journal of Molecular Sciences*, *21*(15), 5443. https://doi.org/10.3390/ijms21155443

[2] Prier, C. K., Rankic, D. A., & MacMillan, D. W. C. (2013). Visible Light Photoredox Catalysis with Transition Metal Complexes: Applications in Organic Synthesis. *Chemical Reviews, 113(7),* 5322–5363. https://doi.org/10.1021/cr300503r

[3] Renfrew, A. K. (2014). Transition metal complexes with bioactive ligands: mechanisms for selective ligand release and applications for drug delivery. *Metallomics, 6(8*), 1324–1335. https://doi.org/10.1039/C4MT00069B

[4] Haiduc, I. (2019). ReviewInverse coordination. Organic nitrogen heterocycles as coordination centers. A survey of molecular topologies and systematization. Part 1. Five-membered and smaller rings. *Journal of Coordination Chemistry, 72,* 2127–2159. https://doi.org/10.1080/00958972.2019.1641702

[5] Mukherjee, R. (2000). Coordination chemistry with pyrazole-based chelating ligands: molecular structural aspects. *Coordination Chemistry Reviews*, *203*(1), 151–218. https://doi.org/10.1016/S0010-8545(99)00144-7

[6] Trofimenko, S. (1986). The Coordination Chemistry of Pyrazole-Derived Ligands. *Progress in Inorganic Chemistry*, *34*, 115–210. https://doi.org/10.1002/9780470166352.ch3

[7] Kupcewicz, B., Sobiesiak, K., Malinowska, K., Koprowska, K., Czyz, M., Keppler, B., Budzisz, E. (2012). Copper(II) complexes with derivatives of pyrazole as potential antioxidant enzyme mimics. *Medicinal Chemistry Research*, *22*(5), 2395–2402. https://doi.org/10.1007/s00044-012-0233-5

[8] Santra, A., Brandao, P., Jana, H., Mondal, G., Bera, P., Jana, A., Bera, P. (2018). Copper(II) and cobalt(II) complexes of 5-methyl pyrazole-3-carboxylic acid: Synthesis, X–ray crystallography, thermal analysis and in vitro antimicrobial activity. *Journal of Coordination Chemistry*, *71*(22) 3648–3664. https://doi.org/10.1080/00958972.2018.1520984

[9] Aljuhani, E., Aljohani, M. M., Alsoliemy, A., Shah, R., Abumelha, H. M., Saad, F. A., Hossan, A., Al-Ahmed, Z. A., Alharbi, A., El-Metwaly, N. M. (2021). Synthesis and Characterization of Cu(II)-Pyrazole Complexes for Possible Anticancer Agents; Conformational Studies as Well as Compatible in-Silico and in-Vitro Assays. *Heliyon*, *7*(11), e08485. https://doi.org/10.1016/j.heliyon.2021.e08485

[10] Zhou, J.-H., Liu, Z., Li, Y.-Z., Song, Y., Chen, X.-T., You, X.-Z. (2006). Synthesis, structures and magnetic properties of two copper(II) complexes with pyrazole and pivalate ligands. *Journal of Coordination Chemistry, 59*(2), *147–156.* https://doi.org/10.1080/00958970500266206

[11] Wiśniewski, M.Z., Głowiak, T. (2000). Copper(II) Methylpyrazole Complexes. *Polish Journal of Chemistry*, *74*(7), 1023–1029. (1293262).

[12] Di Nicola, C., Garau, F., Gazzano, M., Monari, M., Pandolfo, L., Pettinari, C.,Pettinari, R. (2010). Reactions of a Coordination Polymer Based on the Triangular Cluster $[Cu_3(\mu_3\text{-}OH)(\mu\text{-}pz)_3]^{2+}$ with Strong Acids. Crystal

Structure and Supramolecular Assemblies of New Mono-, Tri-, and Hexanuclear Complexes and Coordination Polymers. *Crystal Growth & Design*, *10*(7), 3120–3131. https://doi.org/10.1021/cg1002397

[13] Klingele, J., Dechert, S., Meyer, F. (2009). Polynuclear transition metal complexes of metal···metal-bridging compartmental pyrazolate ligands. *Coordination Chemistry Reviews, 253*(21-22), 2698–2741. https://doi.org/10.1016/j.ccr.2009.03.026

[14] [14] Shi, K., Mathivathanan, L., Boudalis, A. K., Turek, P., Chakraborty, I., & Raptis, R. G. (2019). Nitrite Reduction by Trinuclear Copper Pyrazolate Complexes: An Example of a Catalytic, Synthetic Polynuclear NO Releasing System. *Inorganic Chemistry*, *58(11)*, 7537–7544. https://doi.org/10.1021/acs.inorgchem.9b00748

[15] Bala, S., Akhtar, S., Liu, J.-L., Huang, G.-Z., Wu, S.-G., De, A., Das, K. S., Saha, S., Tong, M.-L., Mondal, R. (2021). Fascinating Interlocked Triacontanuclear Giant Nanocages. *Chemical Communications*, 57(85), 11177–11180. https://doi.org/10.1039/D1CC02990H

[16] Sarma, P., Sharma, P., Frontera, A., Barcelo-Oliver, M., Verma, A. K., Barthakur, T., & Bhattacharyya, M. K. (2021). Unconventional π-hole and Semi-coordination regium bonding interactions directed supramolecular assemblies in pyridinedicarboxylato bridged polymeric Cu(II) Compounds: Antiproliferative evaluation and theoretical studies. *Inorganica Chimica Acta*, *525*, 120461. https://doi.org/10.1016/j.ica.2021.120461

[17] Castro, I., Calatayud, M.L., Orts-Arroyo, M., Moliner, N., Marino, N., Lloret, F., Ruiz-García, R., Munno, G.D., Julve, M. (2021). Ferro- and Antiferromagnetic Interactions in Oxalato-Centered Inverse Hexanuclear and Chain Copper(II) Complexes with Pyrazole Derivatives. *Molecules*, *26*, 2792. https://doi.org/10.3390/molecules26092792

[18] Kokozay, V. N.; Vassilyeva, O. Y.; Makhankova, V. G. (2018). Direct Synthesis of Heterometallic Complexes. In *Direct Synthesis of Metal Complexes*; Kharisov, B., Ed.; Elsevier, 183–237. https://doi.org/10.1016/B978-0-12-811061-4.00005-0

[19] Li, X., Binnemans, K. (2021). Oxidative Dissolution of Metals in Organic Solvents. *Chemical Reviews*, *121*(8), 4506–4530. https://doi.org/10.1021/acs.chemrev.0c00917

[20] Swain, S. P., Kumar, K. N., Mhate, M., Panchami, H., Ravichandiran, V. (2022) Copper (II) Bromide Catalysed One Pot Bromination and Amination for the Green, Cost-Effective Synthesis of Clopidogrel. *Molecular Catalysis*, *522*, 112210. https://doi.org/10.1016/j.mcat.2022.112210

[21] Zai, Y., Feng, Y., Zeng, X., Tang, X., Sun, Y., Lin, L. (2019). Synthesis of 5-aminolevulinic acid with nontoxic regents and renewable methyl levulinate. *RSC Advances*, *9*(18), 10091–10093. https://doi.org/10.1039/C9RA01517E

[22] Moldoveanu, C., Amariucai-Mantu, D., Mangalagiu, V., Antoci, V., Maftei, D., Mangalagiu, I. I., Zbancioc, G. (2019). Microwave Assisted Reactions of Fluorescent Pyrrolodiazine Building Blocks. *Molecules, 24*(20), 3760. https://doi.org/10.3390/molecules24203760

[23] Porré, M., Pisanò, G., Nahra, F., Cazin, C.S.J. (2022). Synthetic Access to Aromatic α-Haloketones. *Molecules*, *27*,3583. https://doi.org/10.3390/molecules27113583

[24] Akhtar, R., Zahoor, A. F., Rasool, N., Ahmad, M., Ali, K. G. (2021). Recent trends in the chemistry of Sandmeyer reaction: a review. *Molecular Diversity*, *26*(3), 1837–1873. https://doi.org/10.1007/s11030-021-10295-3

[25] Rigaku O. D. (2019). *CrysAlisPRO Software system* (ver. 1.171.40.53); Rigaku Oxford Diffraction Ltd: Yarnton, Oxfordshire, England.

[26] Sheldrick, G. M. (2015). SHELXT - Integrated space-group and crystal-structure determination. *Acta Crystallographica Section A*, *71*(1), 3–8. https://doi.org/10.1107/S2053273314026370

[27] Sheldrick G. M. (2015). Crystal structure refinement with SHELXL. *Acta Crystallographica Section C*, *71*, 3–8. https://doi.org/10.1107/S2053229614024218

[28] Dolomanov O. V., Bourhis L. J., Gildea R. J., Howard J. A. K., Puschmann H. (2009). OLEX2: a complete structure solution, refinement and analysis program. *Journal of Applied Crystallography*, *42*, 339–341. https://doi.org/10.1107/S0021889808042726

[29] Clark, R. C., Reid, J. S. (1995). The analytical calculation of absorption in multifaceted crystals. *Acta Crystallographica Section A*, *51*(6), 887–897. https://doi.org/10.1107/S0108767395007367

[30] Spackman, P. R., Turner, M. J., McKinnon, J. J., Wolff, S. K., Grimwood, D. J., Jayatilaka, D. Spackman, M. A. (2021). CrystalExplorer: a program for Hirshfeld surface analysis, visualization and quantitative analysis of molecular crystals. *Journal of Applied Crystallography, 54*(3), 1006–1011. https://doi.org/10.1107/S1600576721002910

[31] Sundaraganesan, N., Kavitha, E., Sebastian, S., Cornard, J. P., Martel, M. (2009). Experimental FTIR, FT-IR (gas phase), FT-Raman and NMR spectra, hyperpolarizability studies and DFT calculations of 3,5-dimethylpyrazole. *Spectrochimica Acta Part A: Molecular and Biomolecular Spectroscopy*, *74*(3), 788–797. https://doi.org/10.1016/j.saa.2009.08.019

[32] Addison, A. W., Rao, T. N., Reedijk, J., van Rijn, J., Verschoor, G. C. (1984). Synthesis, structure, and spectroscopic properties of copper(II) compounds containing nitrogen–sulphur donor ligands; the crystal and molecular structure of aqua[1,7-bis(N-methylbenzimidazol-2′-yl)-2,6-dithiaheptane]copper (II) perchlorate. *Journal of the Chemical Society, Dalton Transactions*, (7), 1349–1356. https://doi.org/10.1039/DT9840001349

[33] Wei, W., Xu, Y. (2012). (*μ*-4-Bromo-3,5-dimethylpyrazolato-*κ*^{2}*N*^{1}:*N*^{2})-*μ*-chlorido-bis[bis(4-bromo-3,5-dimethylpyrazole-*κN*^{2})chloridocopper(II)] acetonitrile monosolvate. *Acta Crystallographica Section E Structure Reports Online, 68*(5), m557. https://doi.org/10.1107/S160053681201402X.